Original Article

Activation of the AKT/GSK-3β/β-catenin pathway via photobiomodulation therapy promotes neural stem cell proliferation in neonatal rat models of hypoxic-ischemic brain damage

Zhaoying Liao, Xuanzi Zhou, Siyu Li, Wei Jiang, Tingsong Li, Nanqing Wang, Nong Xiao

Department of Rehabilitation, Children's Hospital of Chongqing Medical University, National Clinical Research Center for Child Health and Disorders, Ministry of Education Key Laboratory of Child Development and Disorders, China International Science and Technology Cooperation Base of Child Development and Critical Disorders, Chongqing Key Laboratory of Pediatrics, Chongqing Engineering Research Center of Stem Cell Therapy, Chongqing Key Laboratory of Child Health and Nutrition, Chongqing, China

Contributions: (I) Conception and design: N Xiao, W Jiang, Z Liao; (II) Administrative support: None; (III) Provision of study materials or patients: None; (IV) Collection and assembly of data: Z Liao, S Li, X Zhou, N Wang; (V) Data analysis and interpretation: Z Liao, X Zhou; (VI) Manuscript writing: All authors; (VII) Final approval of manuscript: All authors.

Correspondence to: Nong Xiao. Department of Rehabilitation, Children's Hospital of Chongqing Medical University, No. 136 Zhongshan Er Road, Yuzhong District, Chongqing 400014, China. Email: xiaonongwl@163.com.

Background: Hypoxic-ischemic brain damage (HIBD) significantly affects neurodevelopment in infants and is a leading cause of severe neurological morbidity and mortality in neonates. Our previous study found that photobiomodulation therapy (PBMT) improves the impaired spatial learning and memory of HIBD rat models. However, the neuroprotective mechanism conferred by PBMT in HIBD is unclear.

Methods: In the present study, HIBD model rats were treated with PBMT at 5 mW/cm^2 per day in the dark for 14 days (10 min each day), and primary neural stem cells (NSCs) after oxygen-glucose deprivation (OGD) were treated with PBMT for 10 min at 1, 5, 10, and 20 mW/cm^2 in the dark. PBMT promoted hippocampal neural stem cell (NSC) proliferation *in vivo* and *in vitro*.

Results: Mechanistically, PBMT upregulated phosphatidylinositol 3 kinase (PI3K), phosphorylated protein kinase B (p-AKT), phosphorylated glycogen synthase kinase 3 beta (p-GSK-3β), β-catenin, and cyclin D1 expression *in vivo* and *in vitro*, promoting NSC proliferation. Furthermore, both LY294002 (a PI3K inhibitor) and IWR-1 (a Wnt/β-catenin inhibitor) inhibited the PBMT promotion of NSC proliferation after OGD and suppressed β-catenin and cyclin D1 expression *in vitro*.

Conclusions: PBMT improved the spatial learning and memory of HIBD rats and promoted hippocampal NSC proliferation through the AKT/GSK-3β/β-catenin pathway.

Keywords: Hypoxic-ischemic brain damage (HIBD); photobiomodulation therapy (PBMT); spatial learning and memory; proliferation; neural stem cell (NSC)

Submitted Nov 05, 2021. Accepted for publication Jan 07, 2022.
doi: 10.21037/atm-21-5619
View this article at: https://dx.doi.org/10.21037/atm-21-5619

Introduction

Neonatal hypoxic-ischemic brain damage (HIBD) is the most common central nervous system disease in the neonatal period (1). Approximately 20–25% of newborns with HIBD die in the neonatal period, while approximately 25–30% have cognitive impairment (2,3). Currently, treatments for HIBD mainly include supportive therapy and therapeutic hypothermia (4,5), without specific

interventions targeting the underlying pathological changes. Neuronal necrosis and apoptosis begin during the acute phase, followed by neurogenesis in the subacute and recovery phases. Therefore, attenuating neuronal death or promoting neurogenesis may be a novel avenue for interventional therapy for HIBD (6).

Brain photobiomodulation therapy (PBMT) is an innovative physiotherapy for various neurological and psychological diseases (7,8). It has been reported that PBMT can promote neurogenesis in APP/PS1 transgenic mice and thus improve spatial learning and memory (8). In addition, we previously found that 660 nm PBMT improved spatial learning and memory and reduced apoptosis-related molecule synthesis in HIBD model rats, and the biological effect induced by PBMT varied by laser power density (9). To date, little is known about the impact of PBMT on neurogenesis and related molecules in the subacute and recovery phases after HIBD, so we conducted experiments aimed at exploring the impact and its mechanism.

Neuronal proliferation is mainly regulated by the SHH, Notch, Wnt and RA signaling pathways (10,11). The Wnt pathway is highly conserved throughout organismal evolution, and it is thought to play multiple roles in neural stem cell (NSC) self-renewal, embryonic patterning, and neurogenesis in the developing and adult brain (12,13). The Wnt/β-catenin pathway promotes the proliferation of embryonic NSCs under hypoxic or anoxic conditions (14) *in vitro*. Interestingly, our preliminary experiments demonstrated that PBMT upregulated β-catenin expression in NSCs after oxygen-glucose deprivation (OGD) injury. In addition, Jin *et al.* found that PBMT induced protein kinase B (AKT) phosphorylation in hair follicle stem cells and thereby stimulated the Wnt/β-catenin pathway, which ultimately promoted hair follicle stem cell proliferation (15). All of these data suggested that activation of the AKT/glycogen synthase kinase 3 beta (GSK-3β)/β-catenin pathway might be involved in NSC proliferation induced by PBMT in HIBD.

In this study, we conducted *in vivo* and *in vitro* experiments to determine whether PBMT contributes to the rescue of neurocognitive impairment by promoting NSC proliferation in HIBD via the AKT/GSK-3β/β-catenin signaling pathway.

We present the following article in accordance with the ARRIVE reporting checklist (available at https://atm.amegroups.com/article/view/10.21037/atm-21-5619/rc).

Methods

Animals and neonatal HIBD model construction

Sprague-Dawley (SD) rats (8 weeks old) were purchased and housed in a specific pathogen-free (SPF) laboratory at the Experimental Animal Center of Chongqing Medical University [scxk (YU) 2018–0003]. Female rats were mated at a 1:1 ratio, and pregnancy was confirmed. Once the pups were born, 80 7-day-old pups (weighing 15–17 g) were randomly allocated among 4 groups: the sham group, the HIBD group, the sham + PBMT group, and the HIBD + PBMT group (n=20). The HIBD group rats were modeled using the classic Rice method (16): 7-day-old pups underwent surgery in which the left common carotid artery was ligated, and after 30 min of rest, the rats were exposed to a hypoxic environment (8% oxygen + 92% nitrogen) for 2 h. In the sham group, the skin of the neck was incised and sutured, but the artery was not ligated, and rats were not exposed to a hypoxic environment. The experimental procedure is shown in Figure S1A. Experiments were performed under a project license (No. 20200402003) granted by the ethics committee of the Children's Hospital of Chongqing Medical University, in compliance with Chongqing Medical University institutional guidelines for care and use of animals. A protocol was prepared before the study without registration.

Isolation of primary NSCs and OGD

The placentas of the SD rats at 19 days of gestation were stripped free under sterile conditions, and the hippocampal tissues were removed under a dissecting microscope, placed in precooled Dulbecco's Modified Eagle Medium (DMEM), and sheared with ophthalmic scissors. The tissues were blown off the scissors and filtered through a 200-mesh cell sieve. The filtered cell-containing fluid was then centrifuged, and the supernatant was discarded. The sediment layer contained primary NSCs, which were subsequently maintained in DMEM/F12 containing 20 ng/mL basic fibroblast growth factor (bFGF), 20 ng/mL epidermal growth factor (EGF), and 10% B27. The primary NSCs were then cultured in a 10-cm Petri dish and incubated at 37 ℃ with 5% CO_2. The medium was completely changed on the second day of culture and then replaced every other day. Detailed steps of the isolation and characterization of NSCs were previously described (17). On day 6, the cultured primary NSCs were transferred to a 3.5-cm culture dish containing sugar-free M199 and

cultured in a hypoxic incubator (95% N_2 + 5% O_2) for 2 h to induce ischemia and hypoxia. The experimental procedure is shown in Figure S1B,S1C.

PBMT in vivo and in vitro

PBMT was administered as described in our previous work. The SD pups were given PBMT 1 day after HIBD modeling; the head hair was removed, and the rats were fixed on an operating table. Only the rat head was irradiated with 660 nm PBMT from a He-Ne laser, which had been developed and calibrated with a laser power meter at the Institute of Optoelectronics at Nankai University. The transmission of PBMT through the scalp and skull to the hippocampus was measured. PBMT intervention and calibration were completed as described in our previous project (9). During PBMT, the power density of the 660 nm laser to the brain was 5 mW/cm^2, and no local temperature increase in brain tissue was detected. The corresponding laser parameters were as follows: wavelength, 660 nm; optical power density, 5 mW/cm^2; and irradiation duration, 10 min. The pulse parameters were continuous, treatment was administered 14 times, and the treatment frequency was once per day.

Four hours after reoxygenation, primary NSCs were continuously irradiated with a 660 nm laser for 10 min at optical power densities of 1, 5, 10, and 20 mW/cm^2. During the experiment, the cells were maintained in the dark to minimize environmental light interference.

Morris water maze (MWM)

All SD rats were subjected to a MWM test with an MWM system (SLY-WMS 2.0, China) 21 days after HIBD modeling to detect the spatial memory and learning ability of the rats in each group. Detailed steps of the experiment were previously described (9,18).

EdU injections and immunofluorescence

A 5-ethynyl-2'-deoxyuridine (EdU) (RIBBIO, China) test and a Nestin immunofluorescence test were performed to detect the proliferation of hippocampal NSCs on the left side of the brain of the pups in each group. EdU (300 μg/g) was injected into the rats 72 h before being sacrificed, which was 7 days after HIBD modeling. Paraffin-embedded sections of the left side of the brain were prepared. Staining and anti-Nestin antibody marker staining was performed according to the manufacturers' instructions. An inverted fluorescence microscopy system (TE2000-S, Nikon, Japan) was used for imaging, and NIS-Elements AR 3.1 and ImageJ software were used for image analysis.

CCK-8 proliferation assay

Ninety-six-well plates were coated with 0.1 mg/mL polylysine (Sigma-Aldrich, USA) and cleaned 3 times with double distilled H_2O (ddH_2O). Primary NSCs were cultured in prepared 96-well plates (5×10^4 cells/well) for cell counting kit-8 (CCK-8) detection. Each cell group was subjected to OGD when the cell density reached 70–80%, and the PBMT group also received PBMT 4 h after reoxygenation. Ten microliters of CCK-8 solution (Dojindo, Japan) was added to each well for 8, 24, 48, and 72 h after reoxygenation. After CCK-8 incubation with cells at 37 ℃ for 4 h, the absorbance value of each well was measured at 450 nm with a microplate reader.

Flow cytometry was performed to measure the cell cycle

Flow cytometry was performed to analyze the cell cycle of the primary NSCs in each group 24 h after reoxygenation. The primary NSCs were collected and centrifuged at 1,000 rpm for 5 min. Trypsin-EDTA (0.05%) was then added to digest the cells, which were incubated for 5 min at 37 ℃. After digestion was terminated, the cells were gently mixed into suspension 10–20 times. After standing for 2 min, the primary NSC suspension was filtered through a 200-mesh cell sieve, 70% ethanol was added, and the suspension was incubated overnight at 4 ℃ to fix the cells. The fixed cells were washed twice with 0.1 M PBS, 100 μL of RNase A (Solarbio, China) was added, and the cells were then incubated at 37 ℃ for 30 min. Next, 400 μL of propidium iodide (PI) (Solarbio) staining solution was added to the primary NSC suspension and incubated at 4 ℃ for 30 min in the dark. Finally, the proportion of cells in each phase of the cell cycle was determined by flow cytometry (BD FACSCanto, BD Biosciences, USA).

Quantitative real-time polymerase chain reaction (qPCR)

Total RNA was extracted from primary NSCs (24 h after reoxygenation) and the left hippocampus of the rats (7 days after HIBD modeling) using a Simply P Total RNA Extraction kit (BioFlux, China). The extracted RNA

(1,000 ng) was then reverse-transcribed into complementary DNA (cDNA) according to the instructions of the reverse transcription kit (RR047A, TaKaRa, China). Real-time messenger RNA (mRNA) levels were quantified using gene-specific primers and SYBR Green (RR820A, TaKaRa) in a Bio-Rad Laboratories (USA) CFX96 system. The reaction system contained 12.5 μL of SYBR Green, 1 μL of 10 μM PCR forward primer, 1 μL of 10 μM reverse primer, cDNA (10 ng/μL) 2 μL, and 8.5 μL of RNase-free ddH_2O. The primer sequences are shown in Table S1.

Western blot analysis (WB)

According to the instructions of the total protein extraction kit (KGP250, KeyGen Biotech, China), total protein was extracted from primary NSCs (24 h after reoxygenation) and the left hippocampus of the rats (7 days after HIBD modeling). The total extracted protein was quantified using a bicinchoninic assay (BCA) protein detection kit (KGPBCA, KeyGen Biotech). Sodium dodecyl sulphate (SDS)-polyacrylamide gel electrophoresis (10% gel) was then used to isolate the proteins, and the target protein was transferred to a polyvinylidene difluoride (PVDF) membrane. The PVDF membrane was cleaned with tris-buffered saline with Tween (TBST) and sealed with blocking solution for 15 min. After blocking, the primary antibody against the target was added to the membrane and incubated overnight at 4 ℃. The next day, the corresponding secondary antibody was added and incubated at room temperature for 1 h. Finally, an enhanced chemiluminescence (ECL) solution was added to the PVDF membrane and developed with an ECL imaging system (Bio-Rad Laboratories). Images were analyzed with ImageJ software.

Intervention with inhibitors

Phosphatidylinositol 3 kinase (PI3K) inhibitor (LY294002, MCE, USA) and Wnt/β-catenin inhibitor IWR-1 (MCE) were both added to dimethyl sulfoxide (DMSO) and then added to the culture medium 2 h before PBMT.

Statistical analysis

The data are expressed as the mean ± standard error of the mean (SEM). The data were analyzed using SPSS 22.0 statistical software. One-way ANOVA was performed for intergroup comparisons, and the Student-Newman-Keuls (SNK) method was used for intergroup comparisons.

Results

PBMT rescues spatial learning and memory deficits in HIBD SD rats

Compared with those in the sham group, the HIBD model rats showed impaired spatial memory and learning ability. On the first day of assessment, the activity and visual acuity of the rats were ascertained with a visual platform test, and no significant difference in path length or latency time was observed between groups (Figure S2A,S2B). Five days of acquisition training was initiated after the first day of assessment. In representative swimming paths, significant differences between groups were observed on the 5th day of acquisition training (*Figure 1A*). The escape latency and swimming distance of the rats in each group declined during the acquisition period, and this decline was more significant in the HIBD + PBMT group than in the HIBD group as the training progressed (*Figure 1B,1C*), indicating that PBMT rescued the spatial learning of the HIBD rats that had been impaired. After acquisition training, the platform was removed, and the number of times the rats passed the platform area and the time that the rats stayed in the target quadrant were evaluated to assess the spatial memory of the rats. Compared with those in the HIBD group, the rats in the PBMT + HIBD group showed a greater inclination to swim within the target quadrant (*Figure 1D*), and the HIBD rats in the PBMT-treated group passed the platform position more frequently and spent more time in the target quadrant (*Figure 1E,1F*). These results suggested that PBMT can effectively rescue spatial learning and memory deficits in HIBD rats.

PBMT promotes hippocampal NSC proliferation in HIBD SD rats

Neurogenesis in the subacute phase of HIBD is a key factor for neurological repair. After HIBD modeling and PBMT treatment, EdU experiments were performed to detect the proliferation of NSCs in the hippocampus of the rats. As shown in *Figure 2A,2B*, there were significantly more EdU- and nestin-positive cells in the hippocampal dentate gyrus (DG) area of the rats in the HIBD + PBMT group compared with the HIBD group ($P<0.05$), suggesting that PBMT promoted hippocampal NSC proliferation in the HIBD rats and may have attenuated the impaired neurofunction of the HIBD rats.

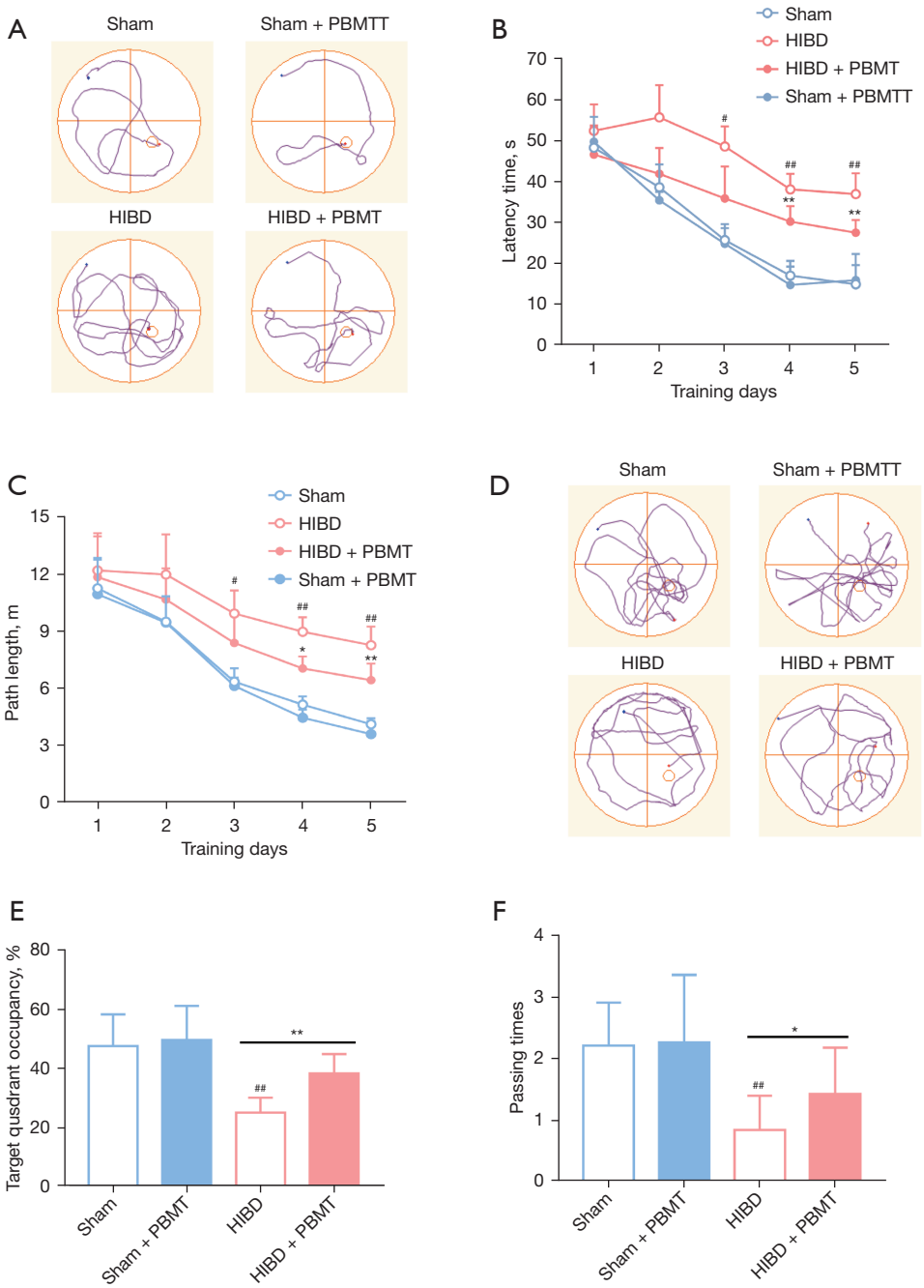

Figure 1 PBMT improves the spatial learning and memory of HIBD rats in the MWM. (A) Representative swimming traces on day 5 during the place navigation trail; (B) the escape latency of SD rats per day to find the hidden platform; (C) mean distance for path length per day to find the hidden platform; (D) representative swimming traces of 4 groups of SD rats after the removal of the resting platform; (E) percentage of time spent in the target quadrant of the original platform position; (F) the number of platform crossings during a 60-s probe trial of the MWM test. The data are reported as the mean ± SEM. N=15 SD rats per group. $^{\#}$P<0.05 and $^{\#\#}$P<0.01 versus the sham group. *P<0.05 and **P<0.01 versus the HIBD group. PBMT, photobiomodulation therapy; HIBD, hypoxic-ischemic brain damage; MWM, Morris water maze; SD, Sprague-Dawley; SEM, standard error of the mean.

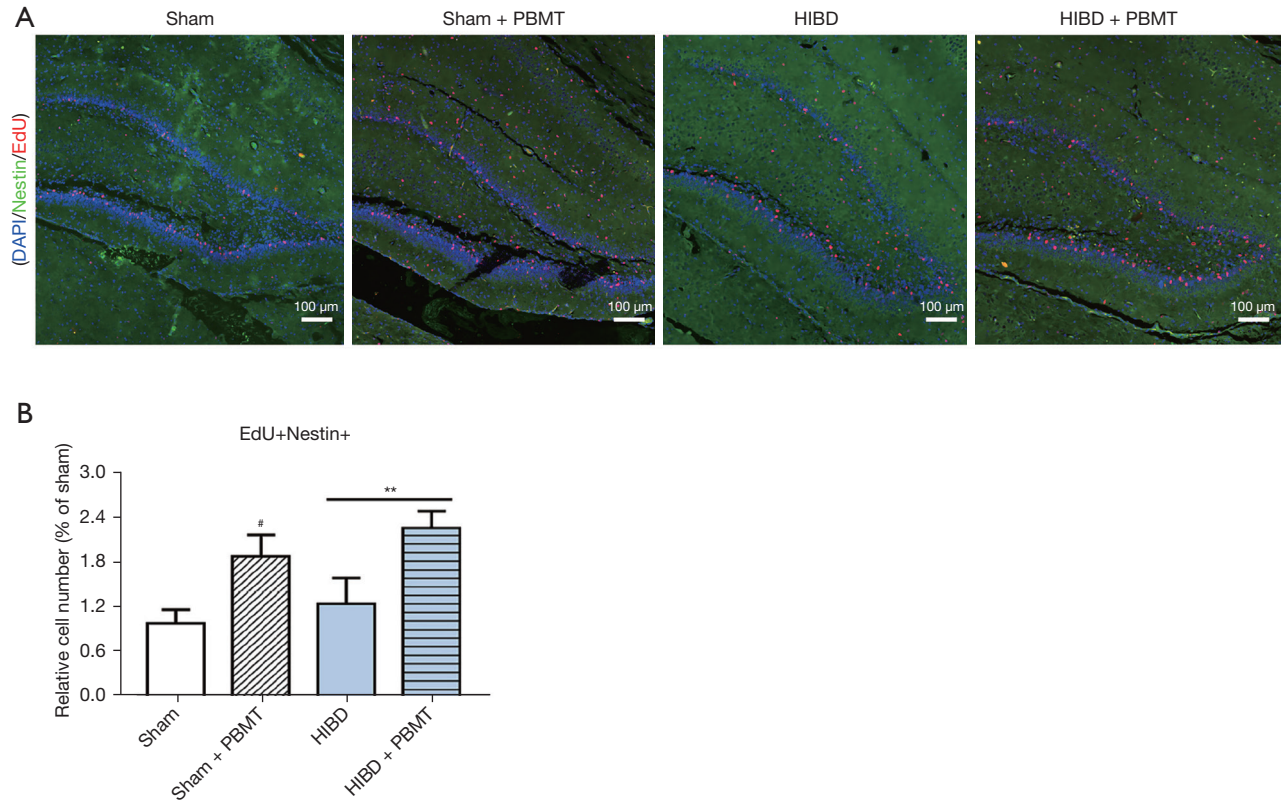

Figure 2 PBMT stimulates hippocampal NSC proliferation in HIBD SD rats. (A) Representative immunofluorescence images of EdU (red)- and Nestin (green)-positive cells in the DG area of the hippocampus after 7 days of HIBD modeling; (B) quantification of the relative numbers of EdU- and Nestin-positive cells in the DG area of the hippocampus. The data are reported as the mean ± SEM. N=5 SD rats per group. #P<0.05 versus the sham group. **P<0.01 versus the HIBD group. PBMT, photobiomodulation therapy; NSC, neural stem cell; HIBD, hypoxic-ischemic brain damage; SD, Sprague-Dawley; DG, dentate gyrus; SEM, standard error of the mean.

PBMT promotes NSC proliferation after OGD in vitro

Previous studies have suggested that PBMT follows a biphasic response based on the applied power density and its biological effect (19,20). In this study, CCK-8 and flow cytometry assays were performed to detect the proliferative effects. As shown in *Figure 3A*, the optical density (OD) values of OGD-injured NSCs treated with PBMT at each time interval were found to be higher than those of OGD-injured NSCs, and the optimal power density threshold was determined to be 5–10 mW/cm^2. Therefore, we chose 10 mW/cm^2 as the intervention power density. Cell cycle analysis (*Figure 3B,3C*) revealed that the percentage of S and G2 phase cells in the OGD + 10 mW/cm^2 PBMT group significantly increased, while the percentage of G1 phase cells decreased (P<0.05). These results suggested that PBMT administered at the appropriate power density can promote OGD-injured NSCs proliferation.

Activation of the GSK-3β/β-catenin pathway by PBMT upregulates cyclin D1 expression and ultimately contributes to hippocampal NSC proliferation in vitro and in vivo

To explore the mechanism through which PBMT promotes the proliferation of hippocampal NSCs in HIBD rats, we screened molecules related to NSC regeneration and found that PBMT upregulated the expression of β-catenin *in vitro* and *in vivo*, and that β-catenin was a critical molecule in neurogenesis. Next, we found that PBMT promoted the transcription of GSK-3β, β-catenin, and cyclin D1 genes in primary NSCs after OGD injury *in vitro* (*Figure 4A*). The *in vitro* WB results (*Figure 4B*) suggested that 10 mW/cm^2 PBMT significantly upregulated the protein expression of phosphorylated GSK-3β (p-GSK-3β), β-catenin, and cyclin D1. With respect to *in vivo* experiments, we found that the mRNA expression level of GSK-3β, β-catenin, and cyclin D1 in the hippocampus of HIBD rats treated with PBMT

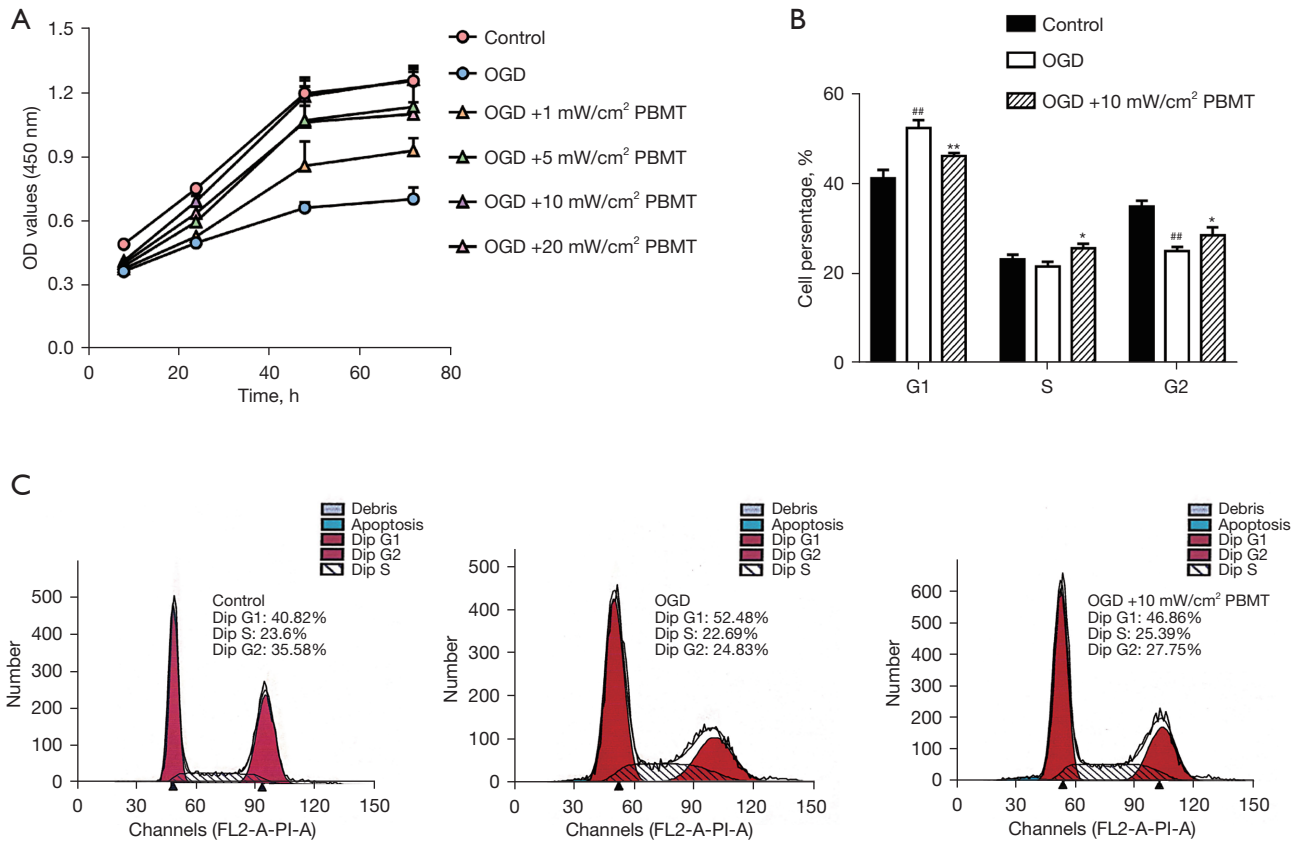

Figure 3 PBMT promotes NSC proliferation in vitro. (A) The effects of different laser power densities on the proliferation of OGD-injured primary NSCs at 8, 24, 48, and 72 h after reoxygenation; (B) Cell cycle analysis of NSCs in different groups; (C) representative flow cytometry DNA histogram in different groups. The data are reported as the mean ± SEM. ##P<0.01 versus the control group. *P<0.05 and **P<0.01 versus the OGD group. PBMT, photobiomodulation therapy; NSC, neural stem cell; OGD, oxygen-glucose deprivation.

was significantly higher than those of HIBD rats (*Figure 4C*, P<0.05). The WB results revealed that after PBMT, the protein expression of p-GSK-3β, β-catenin, and cyclin D1 in the hippocampus of the HIBD rats was significantly increased (*Figure 4D*, P<0.05). These results suggested that PBMT may increase the phosphorylation of GSK-3β, thereby reducing β-catenin degradation in the cytoplasm. β-catenin then promotes the expression of cyclin D1, thereby promoting NSC proliferation.

PBMT stimulates PI3K/AKT pathway activation in vivo and in vitro, leading to GSK-3β/β-catenin activation

Regarding the mechanism through which PBMT activates the GSK-3β/β-catenin pathway, our study found that 660 nm PBMT stimulated the activation of the PI3K/AKT pathway to upregulate the phosphorylation of AKT, and p-AKT then activates the GSK-3β/β-catenin pathway. As shown in *Figure 5A*, the results suggested that PBMT can upregulate the mRNA expression of PI3K and AKT in OGD-injured primary NSCs. The *in vitro* WB results showed (*Figure 5B*) that PBMT upregulated the protein expression of PI3K, AKT, and p-AKT in OGD-injured NSCs, and that the difference was significant when the power density reached 10 mW/cm^2 (P<0.05). With respect to the *in vivo* experiments, the results (*Figure 5C,5D*) revealed that after PBMT, the mRNA and protein expression of PI3K and AKT in the hippocampus of the HIBD rats increased significantly (P<0.05), and the protein expression of p-AKT in the hippocampus of the HIBD rats treated with PBMT was upregulated significantly (P<0.05). These results indicated the potential mechanism through which PBMT stimulates the PI3K/AKT pathway to upregulate the phosphorylation of AKT, which then activates the GSK-3β/β-catenin pathway, thereby inhibiting β-catenin degradation in the cytoplasm. β-catenin then activates cyclin D1 expression to promote NSC proliferation.

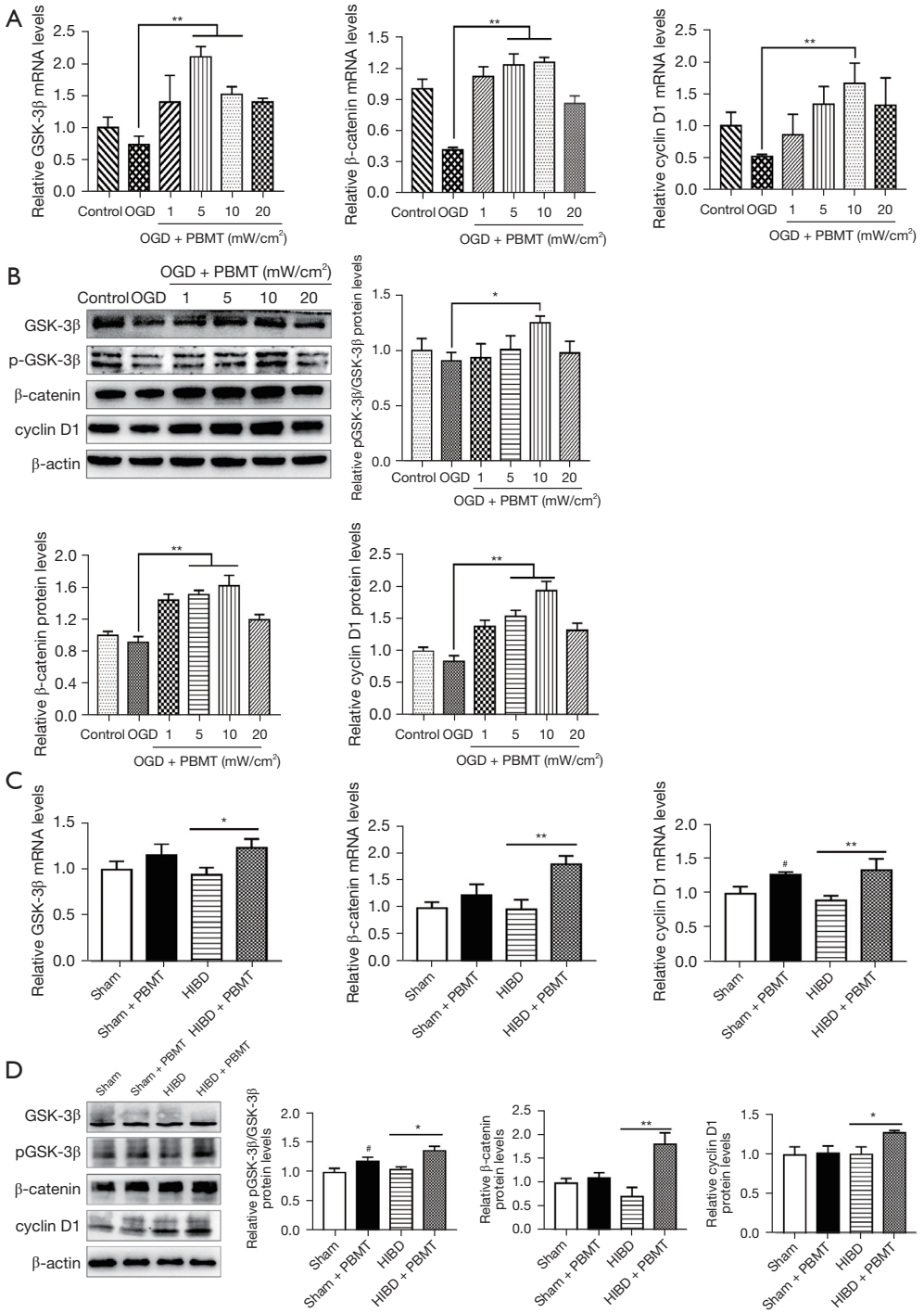

Figure 4 PBMT-induced GSK-3β/β-catenin pathway activation is responsible for NSC proliferation *in vivo* and *in vitro*. (A) The mRNA expression levels of GSK-3β, β-catenin, and cyclin D1 in OGD-injured primary NSCs following PBMT at different power densities *in vitro*; (B) the protein expression levels of GSK-3β, p-GSK-3β, β-catenin, and cyclin D1 in OGD-injured primary NSCs following PBMT at different power densities *in vitro*; (C) the mRNA expression levels of GSK-3β, β-catenin, and cyclin D1 in HIBD SD rats; (D) the protein expression levels of GSK-3β, p-GSK-3β, β-catenin, and cyclin D1 in HIBD SD rats. The data are reported as the mean ± SEM. N=3 SD rats per group. #P<0.05 versus the sham group. *P<0.05 and **P<0.01 versus the indicated group. PBMT, photobiomodulation therapy; NSC, neural stem cell; OGD, oxygen-glucose deprivation; SD, Sprague-Dawley.

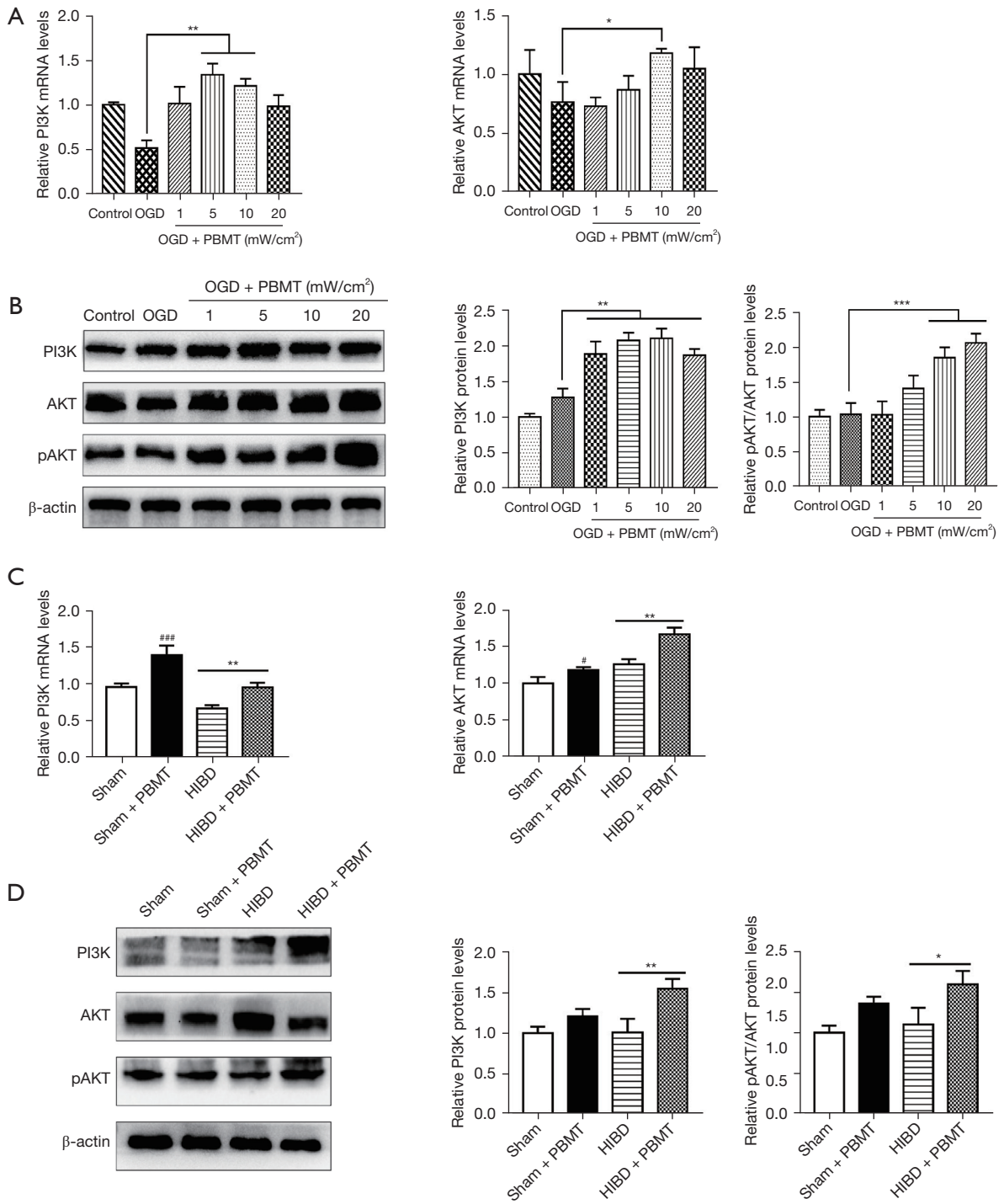

Figure 5 PBMT stimulates the phosphorylation of AKT via the PI3K/AKT pathway and further activates the GSK-3β/β-catenin pathway. (A) The mRNA expression levels of PI3K and AKT in OGD-injured primary NSCs following exposure to PBMT at different power densities *in vitro*; (B) the protein expression levels of PI3K, AKT, and p-AKT in OGD-injured primary NSCs following PBMT at different power densities *in vitro*; (C) the mRNA expression levels of PI3K and AKT in HIBD SD rats; (D) the protein expression levels of PI3K, AKT, and p-AKT in HIBD SD rats. The data are reported as the mean ± SEM. N=3 SD rats per group. $^{\#}$P<0.05 and $^{\#\#\#}$P<0.001 versus the sham group. *P<0.05, **P<0.01, and ***P<0.001 versus the indicated group. PBMT, photobiomodulation therapy; NSC, neural stem cell; OGD, oxygen-glucose deprivation; HIBD, hypoxic-ischemic brain damage; SD, Sprague-Dawley.

LY294002, an inhibitor of PI3K, inhibits the effect of PBMT on NSC proliferation after OGD, suppressing related downstream protein expression

After exploring the potential mechanism through which PBMT promotes the proliferation of OGD-injured NSCs, the mechanism needed to be verified.

As shown in *Figure 6A*, the CCK-8 results indicated that cell viability decreased as the concentration of LY294002 increased, and the difference was significant when the LY294002 concentration reached 10–40 μmol/L ($P<0.05$). On the basis of this finding, we chose 20 μmol/L as the intervention concentration. The results in *Figure 6B* show that the viability of OGD-injured NSCs treated with PBMT was significantly higher than that of OGD-injured NSCs ($P<0.05$). After NSCs were injured by OGD, the cell viability in the 10 mW/cm^2 PBMT + 20 μmol/L LY294002 group was significantly lower than that in the 10 mW/cm^2 PBMT group ($P<0.05$), indicating that LY294002 inhibited NSC proliferation induced by PBMT.

To verify the effect of LY294002 on related downstream molecules, we used qPCR to measure mRNA levels and performed WB and immunofluorescence assays to determine related downstream protein expression.

As shown in *Figure 6C*, the mRNA expression of PI3K, Akt, β-catenin, and cyclin D1 in OGD-injured NSCs treated with PBMT was significantly decreased by pretreatment with 20 μmol/L LY294002 ($P<0.05$). The WB results shown in *Figure 6D* indicated that the expression of PI3K, p-Akt, β-catenin, and cyclin D1 in the LY294002 + PBMT group was significantly reduced compared with that in the PBMT group ($P<0.05$). These results suggested that after LY294002 pretreatment, PBMT-induced activation of the PI3K/Akt signaling pathway was inhibited, resulting in the inhibition of β-catenin and cyclin D1 expression and ultimately, the suppression of NSC proliferation induced by PBMT.

IWR-1, an inhibitor of Wnt/β-catenin, inhibits PBMT promotion of NSC proliferation after OGD and suppresses associated downstream protein expression

We explored the effect of IWR-1, an inhibitor of Wnt/β-catenin, on PBMT-induced NSC proliferation. As shown in *Figure 7A*, the CCK-8 assay results suggested that the best inhibitory concentration of IWR-1 for suppressing the proliferation of NSCs after OGD was 10 μmol/L ($P<0.05$), and therefore, we chose 10 μmol/L as the intervention concentration. As shown in *Figure 7B*, the cell viability of the OGD-injured NSCs treated with PBMT was significantly higher than that of the NSCs in the OGD group ($P<0.05$), and the viability of the NSCs of the IWR-1 + PBMT group was significantly lower than that of the PBMT group ($P<0.05$). These data indicated that IWR-1 inhibited the proliferation of the OGD-injured NSCs that had been induced by PBMT.

As shown in *Figure 7C*, the mRNA expression of GSK-3β, β-catenin, and cyclin D1 in the OGD-injured NSCs treated with PBMT was significantly decreased by pretreatment with 10 μmol/L IWR-1 ($P<0.05$). With regard to protein expression, the WB results (*Figure 7D*) indicated that the expression of GSK-3β, p-GSK-3β, β-catenin, and cyclin D1 in the IWR-1 + PBMT group was significantly reduced compared with that in the PBMT group ($P<0.05$). These results indicated that IWR-1 inhibited PBMT-induced activation of the GSK-3β/β-catenin pathway, thereby downregulating β-catenin and cyclin D1 expression and ultimately inhibiting the proliferative effect of PBMT.

Discussion

To our knowledge, this study is the first to show that 660 nm PBMT promoted the proliferation of NSCs in the hippocampus of rats during the subacute phases of HIBD, improving the spatial memory and learning ability of HIBD rats. This study validates findings indicating that PBMT induces AKT phosphorylation, leading to the phosphorylation of GSK-3β after HIBD injury in the subacute and recovery phases. This increase in p-GSK-3β inhibits the degradation of β-catenin in the cytoplasm. Therefore, the accumulated β-catenin activates cyclin D1 transcription and promotes hippocampal NSC proliferation, thereby achieving neurological repair. The mechanism described in this study is shown in diagram form in *Figure 8*. In summary, PBMT could be a new potential treatment for neonatal HIBD, and it may represent a viable means to promote hippocampal NSC proliferation in subacute and recovery phases of neonatal HIBD, ameliorating cognitive impairments caused by HIBD and further prognosis.

HIBD is the most common central nervous system disease in newborns, with a prevalence of 1–8% in developed countries and 14.9–26% in developing countries (1). Dyskinesia and neurodevelopmental disorders can remain after moderate and severe HIBD. The only current therapeutic intervention for HIBD is therapeutic hypothermia, but its curative effect is limited. The cascades of oxidative metabolism and apoptosis in the early stage

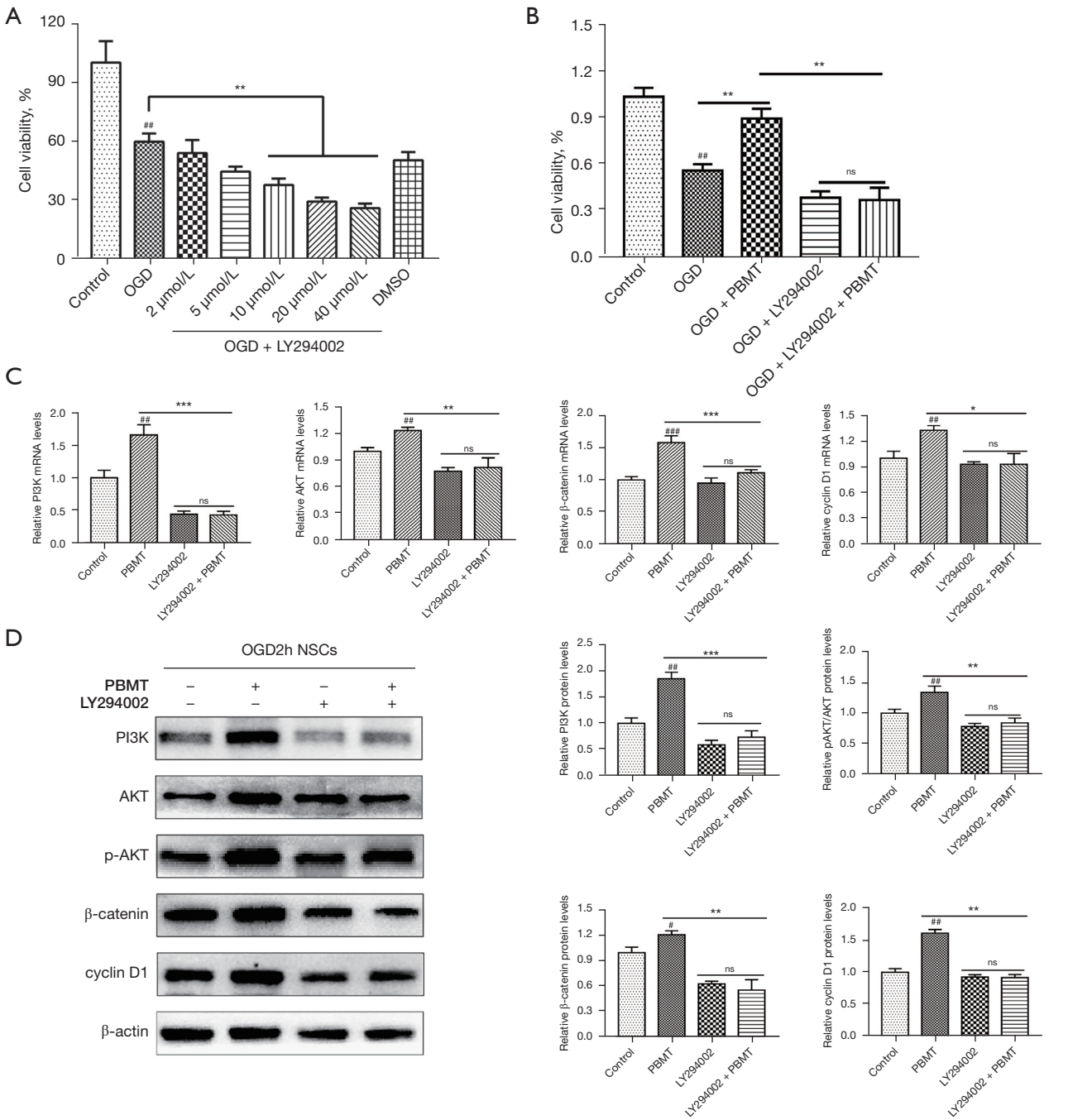

Figure 6 LY294002 (PI3K inhibitor) inhibited the PBMT-induced proliferation of primary NSCs after OGD and inhibited the expression of downstream related proteins. (A) Intervention concentration of PI3K inhibitor LY294002; (B) comparison of proliferation detection in each group of primary NSCs after OGD; (C) the mRNA expression levels of PI3K, AKT, GSK-3β, β-catenin, and cyclin D1 after treatment with PBMT (10 mW/cm^2) in the presence of LY294002 (20 μM) in OGD-injured primary NSCs; (D) the protein expression levels of PI3K, AKT, p-AKT, β-catenin, and cyclin D1 after treatment with PBMT (10 mW/cm^2) in the presence of LY294002 (20 μM) in OGD-injured primary NSCs. The data are reported as the mean ± SEM. $^{\#}$P<0.05, $^{\#\#}$P<0.01, and $^{\#\#\#}$P<0.001 versus the control group. *P<0.05, **P<0.01, and ***P<0.001 versus the indicated group. + group treated with indicated intervention, – group treated without indicated intervention. PBMT, photobiomodulation therapy; NSC, neural stem cell; OGD, oxygen-glucose deprivation; HIBD, hypoxic-ischemic brain damage; SEM, standard error of the mean.

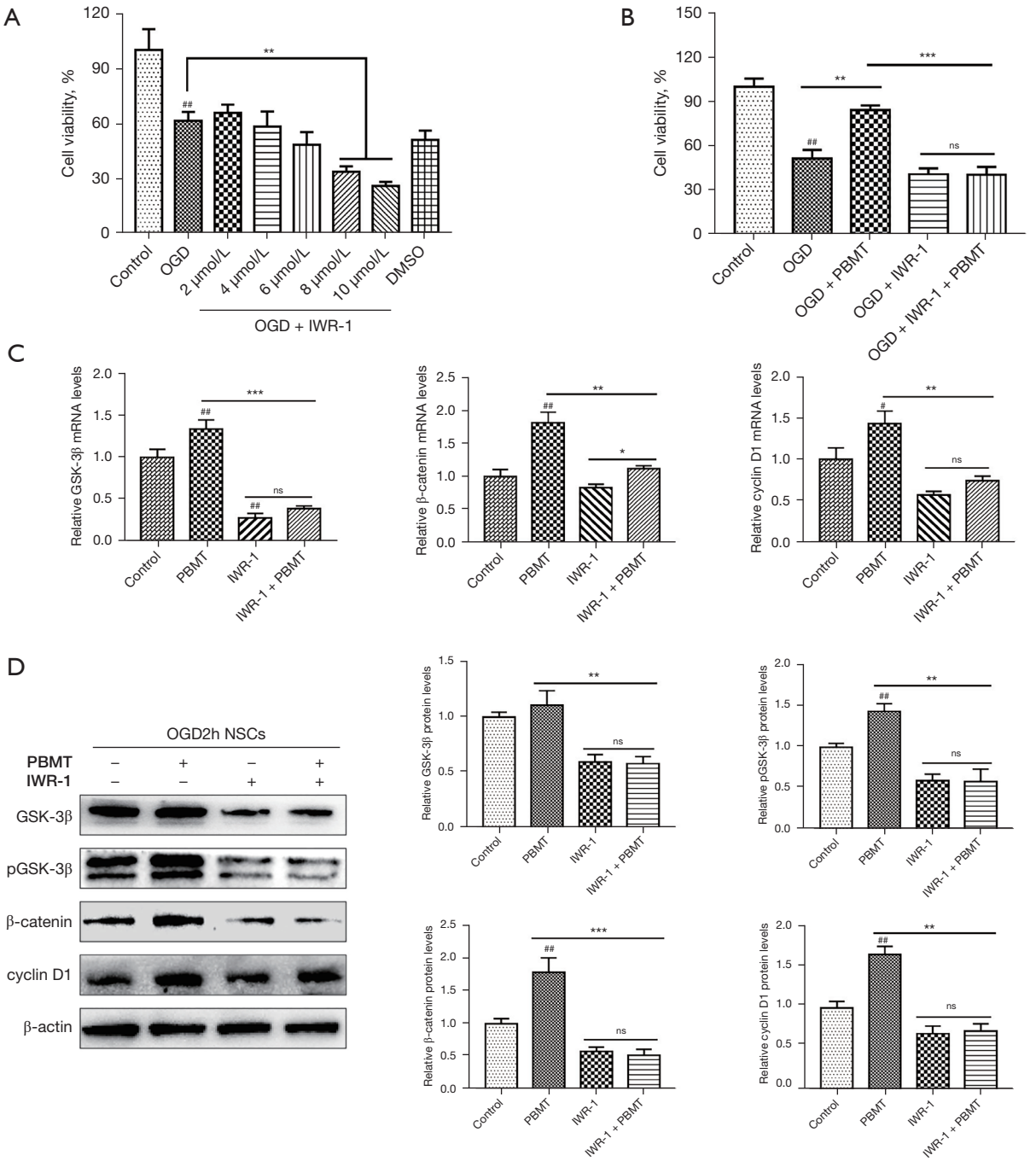

Figure 7 IWR-1 (Wnt/β-catenin inhibitor) inhibited the PBMT-induced proliferation of primary NSCs after OGD and inhibited the expression of downstream related proteins. (A) Intervention concentration of the Wnt/β-catenin inhibitor IWR-1; (B) comparison of proliferation detection in each group of primary NSCs after OGD; (C) the mRNA expression levels of GSK-3β, β-catenin, and cyclin D1 after treatment with PBMT (10 mW/cm^2) in the presence of IWR-1 (10 μM) in OGD-injured primary NSCs; (D) the protein expression levels of GSK-3β, p-GSK-3β, β-catenin, and cyclin D1 after treatment with PBMT (10 mW/cm^2) in the presence of IWR-1 (10 μM) in OGD-injured primary NSCs. The data are reported as the mean ± SEM. $^{\#}$P<0.05 and $^{\#\#}$P<0.01 versus the control group. *P<0.05, **P<0.01, and ***P<0.001 versus the indicated group. + group treated with indicated intervention, – group treated without indicated intervention. PBMT, photobiomodulation therapy; NSC, neural stem cell; OGD, oxygen-glucose deprivation; SEM, standard error of the mean.

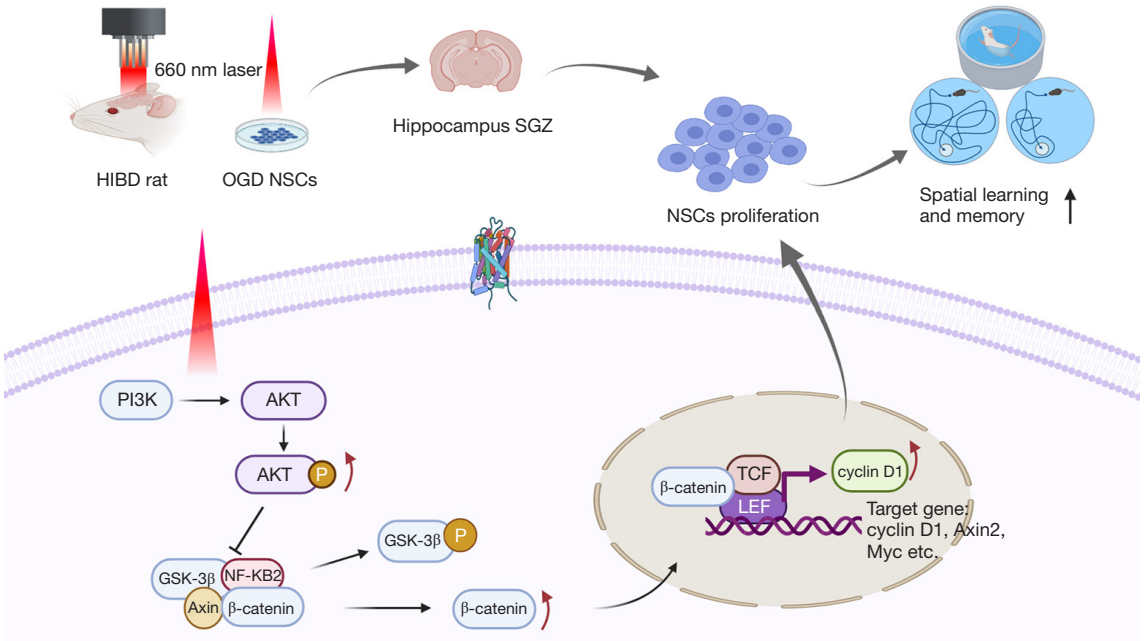

Figure 8 Schematic representation showing that photoactivation of the AKT/GSK-3β/β-catenin signaling pathway promotes hippocampal NSC proliferation in a neonatal HIBD model. HIBD, hypoxic-ischemic brain damage; NSC, neural stem cell; SGZ, subgranular zone; TCF, T cell factor; LEF, lymphoid enhancer factor; Axin2, Axis inhibition protein 2; Myc, MYC proto-Oncogene.

of the pathological HIBD process (within 6 h) lead to cell necrosis and apoptosis, with the apoptosis rate peaking at 48–72 h. In the subacute phase (6–48 h) and the recovery phase, damaged brain remodeling and proliferation of NSCs and astrocytes begin to appear. Neurogenesis in this period is also one of the keys to neurological repair (6,21). Therefore, it is necessary to explore new possible treatment measures for use during the critical period of HIBD neurological remodeling.

Brain PBMT is an innovative treatment method for neuropsychological diseases that is based on low-level red light or infrared light. Previous studies have shown that PBMT stimulates anti-inflammatory, antiapoptotic, and antioxidant actions, nerve regeneration, and synapse formation, and therefore, PBMT has been used to treat dementia, Alzheimer's disease, brain trauma, and depression (22,23). There are other physiotherapies which have therapeutic effect of HIBD in previous studies like therapeutic hypothermia and hyperbaric oxygen therapy (6,24), whose therapeutic effect are mainly about anti-apoptosis or anti-inflammation in acute phase (within 6 h) after HIBD. While in this study, we mainly focused on neurogenesis of PBMT during the subacute and recovery phase after HIBD. The proliferation and differentiation of NSCs are critical to HIBD neurological repair. In newborn rats, the proliferation and differentiation of NSCs in the hippocampus are key to the restoration of cognitive function in HIBD rats (3,25,26). As expected, we found that 660 nm PBMT improved the impaired spatial memory and learning ability of HIBD rats. In addition, this study confirmed that PBMT can promote NSC proliferation in the hippocampal DG region after HIBD modeling in SD rats, and that 5–10 mW/cm^2 PBMT can also promote OGD-injured NSC proliferation *in vitro*.

Our research found that PBMT activated the PI3K/AKT pathway in NSCs of the hippocampus in HIBD rats. The PI3K/AKT signaling pathway regulates the proliferation and differentiation of stem cells upon hypoxic injury (27) and regulates the apoptosis and autophagy of neurons during hypoxic-ischemic injury (28). PBMT activated the PI3K/AKT pathway, induced the phosphorylation of AKT, regulated downstream molecules, and ultimately promoted the proliferation of NSCs after OGD injury. In contrast, the PI3K inhibitor LY294002 inhibited the proliferative effect induced by PBMT, thus verifying the effect of the PI3K/AKT pathway in PBMT.

The AKT signaling pathway plays an important cell biological function and can inhibit the activation of GSK-

3β (29). In addition, we found that PBMT significantly upregulated the expression of β-catenin in OGD-injured hippocampal NSCs. The maintenance of a functional circuit requires a balance between NSC proliferation and neural differentiation, which is largely dependent on the physiological activation of the Wnt pathway (12,30). The disruption of NSC homeostasis through the modulation of the Wnt/β-catenin pathway leads to the pathogenesis involved in various neurological diseases (31), and β-catenin plays an important role in neurogenesis and neurological repair. The Wnt/β-catenin pathway can promote the proliferation and regulation of NSCs in hypoxic-ischemic injury (14,32). Notably, Wnt/β-catenin signaling is a potential therapeutic target for the treatment of neurological disease. In nerve repair, when Wnt protein binds to receptors [namely, Frizzled protein and lipoprotein receptor-related protein (LRP) 5/6], the signal is transmitted through the cell by phosphorylated disheveled protein to inhibit adenomatous polyposis coli (APC) expression. GSK-3β, Axin, and β-catenin constitute a kinase complex that inhibits the degradation of β-catenin, causing activated β-catenin accumulation in the cytoplasm. A portion of this β-catenin enters the nucleus where it combines with T cell factor (TCF) and lymphoid enhancer factor (LEF), and in conjunction with other cellular factors, releases the inhibited state induced by LEF/TCF, activating the transcription of downstream target genes cyclin Dl, Axin2, Sox9, and Lef-1 (33). Cyclin D1 is a key protein in cell cycle proliferation signaling, which is necessary for the cell cycle transition, and upregulation of cyclin D1 expression can further promote the proliferation of NSCs (34). In this study, we found that PBMT activated the GSK-3β/β-catenin pathway in HIBD model rats and upregulated the expression of β-catenin and cyclin D1 to promote NSC proliferation. The Wnt/β-catenin inhibitor IWR-1 inhibited this proliferative effect, verifying our hypothesis.

Our study had several limitations. First, we did not reverse verify the AKT/GSK-3β/β-catenin pathway *in vivo* because we have not successfully established a rat model that can stably inhibit AKT or GSK phosphorylation of NSCs in the hippocampus. In addition, the mechanism through which PBMT activates the PI3K/AKT pathway remains unknown. Further, the differentiation of NSCs is an important aspect of neurogenesis and neurological repair, but it was not investigated in our study. All of the above issues require further study.

We found that PBMT improved the spatial memory and learning ability of HIBD rats. The potential reason is based on PBMT activation of the AKT/GSK-3β/β-catenin pathway in the subacute phase of HIBD, which promoted NSC proliferation in the hippocampus of HIBD rats. Combined with the early findings of our research group showing that PBMT exerts an antiapoptotic effect in the acute phase of HIBD, PBMT may be a new therapeutic strategy for HIBD.

Acknowledgments

We thank all of the participants for their help.
Funding: This work was supported by the Nature Science Foundation of China (81541033 for N Xiao).

Footnote

Reporting Checklist: The authors have completed the ARRIVE reporting checklist. Available at https://atm.amegroups.com/article/view/10.21037/atm-21-5619/rc

Data Sharing Statement: Available at https://atm.amegroups.com/article/view/10.21037/atm-21-5619/dss

Conflicts of Interest: All authors have completed the ICMJE uniform disclosure form (available at https://atm.amegroups.com/article/view/10.21037/atm-21-5619/coif). N Xiao reports funding from the Nature Science Foundation of China (81541033). The other authors have no conflicts of interest to declare.

Ethical Statement: The authors are accountable for all aspects of the work in ensuring that questions related to the accuracy or integrity of any part of the work are appropriately investigated and resolved. Experiments were performed under a project license (No. 20200402003) granted by the ethics committee of the Children's Hospital of Chongqing Medical University, in compliance with Chongqing Medical University institutional guidelines for care and use of animals.

References

1. Douglas-Escobar M, Weiss MD. Hypoxic-ischemic encephalopathy: a review for the clinician. JAMA Pediatr 2015;169:397-403.
2. Dumbuya JS, Chen L, Wu JY, et al. The role of G-CSF neuroprotective effects in neonatal hypoxic-ischemic encephalopathy (HIE): current status. J Neuroinflammation 2021;18:55.
3. Logitharajah P, Rutherford MA, Cowan FM. Hypoxic-ischemic encephalopathy in preterm infants: antecedent factors, brain imaging, and outcome. Pediatr Res 2009;66:222-9.
4. Laptook AR, Shankaran S, Tyson JE, et al. Effect of Therapeutic Hypothermia Initiated After 6 Hours of Age on Death or Disability Among Newborns With Hypoxic-Ischemic Encephalopathy: A Randomized Clinical Trial. JAMA 2017;318:1550-60.
5. Finder M, Boylan GB, Twomey D, et al. Two-Year Neurodevelopmental Outcomes After Mild Hypoxic Ischemic Encephalopathy in the Era of Therapeutic Hypothermia. JAMA Pediatr 2020;174:48-55.
6. Yildiz EP, Ekici B, Tatli B. Neonatal hypoxic ischemic encephalopathy: an update on disease pathogenesis and treatment. Expert Rev Neurother 2017;17:449-59.
7. Tucker LD, Lu Y, Dong Y, et al. Photobiomodulation Therapy Attenuates Hypoxic-Ischemic Injury in a Neonatal Rat Model. J Mol Neurosci 2018;65:514-26.
8. Wu X, Shen Q, Zhang Z, et al. Photoactivation of TGFbeta/SMAD signaling pathway ameliorates adult hippocampal neurogenesis in Alzheimer's disease model. Stem Cell Res Ther 2021;12:345.
9. Jiang W, Chen L, Zhang XJ, et al. Red photon treatment inhibits apoptosis via regulation of bcl-2 proteins and ROS levels, alleviating hypoxic-ischemic brain damage. Neuroscience 2014;268:66-74.
10. Ferreira R, Fonseca MC, Santos T, et al. Retinoic acid-loaded polymeric nanoparticles enhance vascular regulation of neural stem cell survival and differentiation after ischaemia. Nanoscale 2016;8:8126-37.
11. Zhang J, Kang N, Yu X, et al. Radial Extracorporeal Shock Wave Therapy Enhances the Proliferation and Differentiation of Neural Stem Cells by Notch, PI3K/AKT, and Wnt/beta-catenin Signaling. Sci Rep 2017;7:15321.
12. Bond AM, Ming GL, Song H. Adult Mammalian Neural Stem Cells and Neurogenesis: Five Decades Later. Cell Stem Cell 2015;17:385-95.
13. Clevers H, Loh KM, Nusse R. Stem cell signaling. An integral program for tissue renewal and regeneration: Wnt signaling and stem cell control. Science 2014;346:1248012.
14. Qi C, Zhang J, Chen X, et al. Hypoxia stimulates neural stem cell proliferation by increasing HIF1alpha expression and activating Wnt/beta-catenin signaling. Cell Mol Biol (Noisy-le-grand) 2017;63:12-9.
15. Jin H, Zou Z, Chang H, et al. Photobiomodulation therapy for hair regeneration: A synergetic activation of beta-CATENIN in hair follicle stem cells by ROS and paracrine WNTs. Stem Cell Reports 2021;16:1568-83.
16. Rice JE, 3rd, Vannucci RC, Brierley JB. The influence of immaturity on hypoxic-ischemic brain damage in the rat. Ann Neurol 1981;9:131-41.
17. Gage FH, Ray J, Fisher LJ. Isolation, characterization, and use of stem cells from the CNS. Annu Rev Neurosci 1995;18:159-92.
18. Vorhees CV, Williams MT. Morris water maze: procedures for assessing spatial and related forms of learning and memory. Nat Protoc 2006;1:848-58.
19. Sharma SK, Kharkwal GB, Sajo M, et al. Dose response effects of 810 nm laser light on mouse primary cortical neurons. Lasers Surg Med 2011;43:851-9.
20. Xuan W, Huang L, Hamblin MR. Repeated transcranial low-level laser therapy for traumatic brain injury in mice: biphasic dose response and long-term treatment outcome. J Biophotonics 2016;9:1263-72.
21. Wang Q, Lv H, Lu L, et al. Neonatal hypoxic-ischemic encephalopathy: emerging therapeutic strategies based on pathophysiologic phases of the injury. J Matern Fetal Neonatal Med 2019;32:3685-92.
22. Lu Y, Wang R, Dong Y, et al. Low-level laser therapy for beta amyloid toxicity in rat hippocampus. Neurobiol Aging 2017;49:165-82.
23. Ramezani F, Neshasteh-Riz A, Ghadaksaz A, et al. Mechanistic aspects of photobiomodulation therapy in the nervous system. Lasers Med Sci 2021. [Epub ahead of print]. doi: 10.1007/s10103-021-03277-2.
24. Zhai X, Lin H, Chen Y, et al. Hyperbaric oxygen preconditioning ameliorates hypoxia-ischemia brain damage by activating Nrf2 expression in vivo and in vitro. Free Radic Res 2016;50:454-66.
25. Toda T, Parylak SL, Linker SB, et al. The role of adult hippocampal neurogenesis in brain health and disease. Mol Psychiatry 2019;24:67-87.
26. Tang C, Wang M, Wang P, et al. Neural Stem Cells Behave as a Functional Niche for the Maturation of Newborn Neurons through the Secretion of PTN.

Neuron 2019;101:32-44 e6.
27. Kisoh K, Hayashi H, Arai M, et al. Possible Involvement of PI3-K/Akt-Dependent GSK-3beta Signaling in Proliferation of Neural Progenitor Cells After Hypoxic Exposure. Mol Neurobiol 2019;56:1946-56.
28. Wei W, Lu M, Lan XB, et al. Neuroprotective Effects of Oxymatrine on PI3K/Akt/mTOR Pathway After Hypoxic-Ischemic Brain Damage in Neonatal Rats. Front Pharmacol 2021;12:642415.
29. Zheng R, Zhang ZH, Chen C, et al. Selenomethionine promoted hippocampal neurogenesis via the PI3K-Akt-GSK3beta-Wnt pathway in a mouse model of Alzheimer's disease. Biochem Biophys Res Commun 2017;485:6-15.
30. Lie DC, Colamarino SA, Song HJ, et al. Wnt signalling regulates adult hippocampal neurogenesis. Nature 2005;437:1370-5.
31. Noelanders R, Vleminckx K. How Wnt Signaling Builds the Brain: Bridging Development and Disease. Neuroscientist 2017;23:314-29.
32. Arredondo SB, Valenzuela-Bezanilla D, Mardones MD, et al. Role of Wnt Signaling in Adult Hippocampal Neurogenesis in Health and Disease. Front Cell Dev Biol 2020;8:860.
33. Gao J, Liao Y, Qiu M, et al. Wnt/beta-Catenin Signaling in Neural Stem Cell Homeostasis and Neurological Diseases. Neuroscientist 2021;27:58-72.
34. Bragado Alonso S, Reinert JK, Marichal N, et al. An increase in neural stem cells and olfactory bulb adult neurogenesis improves discrimination of highly similar odorants. EMBO J 2019;38:e98791.

Cite this article as: Liao Z, Zhou X, Li S, Jiang W, Li T, Wang N, Xiao N. Activation of the AKT/GSK-3β/β-catenin pathway via photobiomodulation therapy promotes neural stem cell proliferation in neonatal rat models of hypoxic-ischemic brain damage. Ann Transl Med 2022;10(2):55. doi: 10.21037/atm-21-5619

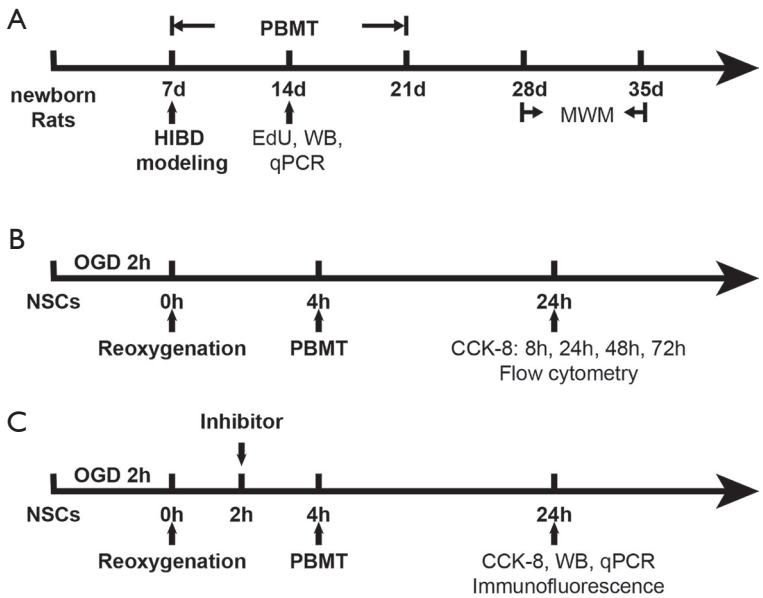

Figure S1 Experimental procedures *in vivo* and *in vitro*. PBMT, photobiomodulation therapy; NSC, neural stem cell; OGD, oxygen-glucose deprivation; MWM, Morris water maze; qPCR, quantitative real-time polymerase chain reaction; WB, Western blot; EdU, 5-ethynyl-2'-deoxyuridine; CCK-8, cell counting kit-8.

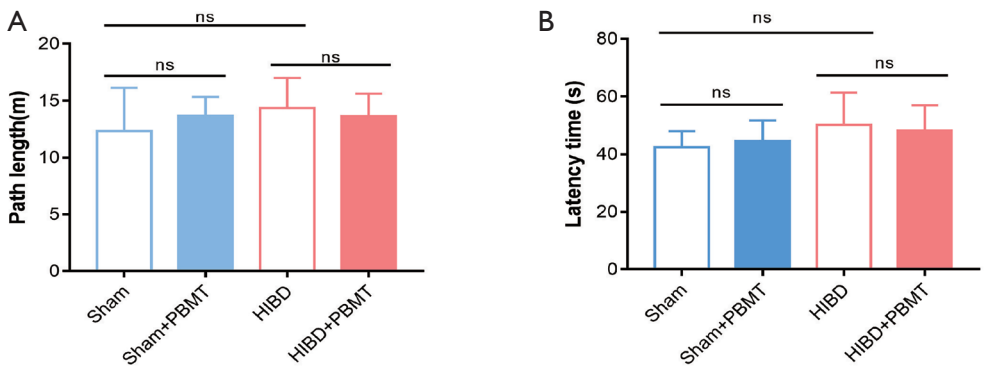

Figure S2 Cognitive function of rats in different groups. (A) The path length of rats in different groups in the Morris water maze (MWM) experiment with a visual platform; (B) the latency time of rats in different groups in the MWM experiment with a visual platform. ns no statistical significance versus the indicated group. PBMT, photobiomodulation therapy; HIBD, hypoxic-ischemic brain damage.

https://dx.doi.org/10.21037/atm-21-5619

Table S1 The related primer sequences in this study

Primer name	Primer sequence
PI3K	F: CTGGAAGCCATTGAGAAG
	R: CAGGATTTGGTAAGTCGG
Akt	F: TGAGACCGACACCAGGTATTTTG
	R: GCTGAGTAGGAGAACTGGGGAAA
GSK-3β	F: CATCCTTATCCCTCCTCACGCT
	R: TATTGGTCTGTCCACGGTCTCC
β-catenin	F: GTTCTACGCCATCACGACAC
	R: GAGCAGACAAGCACTTTC
Cyclin D1	F: TTCATCGAACACTTCCTCTCCA
	R: GAGGGTGGGTTGGAAATGAA
GAPDH	F: CTGGAGAAACCTGCCAAGTATG
	R: GGTGGAAGAATGGGAGTTGCT

https://dx.doi.org/10.21037/atm-21-5619